

- C. D. Wagner, W. M. Riggs, L. E. Davis, J. F. Moulder, G. E. Muilenberg, Eds. (Perkin-Elmer Corporation, Eden Prairie, MN, 1979), p. 40.
15. Film adhesion was measured qualitatively with an adhesive tape test. Pieces of adhesive tape were attached to the surfaces of the C-N and C films and then peeled off these surfaces. No material was removed from surfaces of the C-N films; however, significant solid was peeled from C sample surfaces. These results are indicative of good adhesion and poor adhesion, respectively. In addition, we found that dragging a hard metal needle across the surface of the C-N films does not produce observable damage, although dragging this needle across the C films produces a deep groove. Future studies of microindentation will be needed, however, to assess quantitatively the film hardness.
  16. We have further probed the structure of these films using convergent beam electron diffraction. These preliminary data, which were obtained on individual crystallites within the films, are consistent with the  $\beta$ - $C_3N_4$  structure. Single crystal materials will be needed, however, to fully resolve the structure of these C-N materials with four-circle x-ray diffraction.
  17. We believe that there are several experimental factors that may be explored in the future to increase further the average nitrogen content of

the films. First, a higher RF discharge power would increase the dissociation fraction and kinetic energy of the N atoms in the beam. Both of these effects should increase the extent of reaction with the carbon fragments and thereby increase the average N content in the films. At present, however, our atomic beam source cannot be operated at  $>150$  W used in this study. Secondly, we believe that it will be important to control better the sizes of the carbon fragments produced by laser ablation since larger carbon fragments may not react completely with the atomic nitrogen beam. Variations in the laser power density and photofragmentation of the ablated carbon species are two strategies that we are currently using to study how the carbon fragment size affects the extent of reaction with atomic nitrogen.

18. We acknowledge J. E. Pollard for helpful discussions and D. R. Herschbach for the loan of the diffusion pumps used in these studies. C.M.L. acknowledges support of this work through a National Science Foundation–Presidential Young Investigator award and the NSF-supported Materials Research Laboratory at Harvard.

10 May 1993; accepted 4 June 1993

## Interlayer Tunneling and Gap Anisotropy in High-Temperature Superconductors

Sudip Chakravarty, Asle Sudbø, Philip W. Anderson, Steven Strong

A quantitative analysis of a recent model of high-temperature superconductors based on an interlayer tunneling mechanism is presented. This model can account well for the observed magnitudes of the high transition temperatures in these materials and implies a gap that does not change sign, can be substantially anisotropic, and has the same symmetry as the crystal. The experimental consequences explored so far are consistent with the observations.

The gap in the electronic spectrum at the Fermi energy is a distinguishing feature of a superconductor; it is also the order parameter that describes the broken symmetry of the superconducting phase. The macroscopic properties of a superconductor follow once the gap is known. Here we explore a gap equation that was recently proposed by one of us (1) to explain the properties of the high-temperature cuprate superconductors. The underlying mechanism that leads to this gap equation is an interlayer tunneling phenomenon. We show (i) that the high transition temperatures of these materials can be natural consequences of this mechanism, (ii) that the superconducting gap can exhibit substantial anisotropy similar to that observed in recent photoemission measurements (2) but does not change sign (it is not possible to detect the sign of the gap in photoemission experiments), and (iii) that the superconducting state does not

exhibit a Hebel-Slichter peak in the nuclear magnetic relaxation rate. Because the gap does not change sign and has the same symmetry as the crystal, even a moderate amount of nonmagnetic impurity scattering is likely to have little effect on the superconducting transition temperature  $T_c$ . We refer to this gap as an anisotropic  $s$ -wave gap.

The interlayer tunneling mechanism (1) is based on the presence of well-defined CuO layers in these materials. The idea is to amplify the pairing mechanism within a given layer by allowing the Cooper pairs to tunnel to an adjacent layer by the Josephson mechanism. This delocalization process of the pairs gives rise to a substantial enhancement of pairing only if the coherent single particle tunneling between the layers is blocked, which we argue to be the case on phenomenological as well as theoretical grounds. In this sense the presence of bilayers or triple layers in these materials is important. The principle of amplification, however, is indifferent to the specific mechanism within a given CuO layer; the pairing can be due to electron-phonon interaction

or spin fluctuations (3). We shall assume that the electron-phonon interaction is the dominant mechanism. As shown below, this leads to a natural explanation of the anomalous isotope effect seen in these materials. It is known that the isotope effect is negligibly small for materials with the highest  $T_c$ 's and reverts to near normal for very low ones.

The normal state of these materials exhibits properties that require us to go beyond the conventional Fermi liquid theory (4). Here we assume that, owing to strong electronic correlation effects, coherent single particle tunneling is not possible between the adjacent layers of a given bilayer even though the bare hopping rate, as obtained from electronic structure calculations, is substantial, of the order of 0.1 eV—a phenomenon that has been termed confinement (1). To justify this assumption, we briefly recall the phenomenology of the normal state of the high-temperature superconductors; for a more complete discussion, see (4).

Suppose for the moment that the normal state is described by a Fermi liquid. Then, the two CuO layers hybridized by the single particle tunneling matrix element,  $t_{\perp}(\mathbf{k})$ , would lead to a symmetric and an antisymmetric combination of the quasiparticle states for each value of the wave vector  $\mathbf{k}$  in the plane. (Throughout this report,  $\mathbf{k}$  will refer to a two-dimensional wave vector.) Because these states are dipole-active, the transition between them should lead to a prominent signature in the frequency-dependent  $c$ -axis conductivity, which, to date, has not been observed. [Because of the  $\mathbf{k}$  dependence of  $t_{\perp}(\mathbf{k})$ , the signature is likely to be broad, but should still be observable in the range 500 to 1000  $\text{cm}^{-1}$ .] In contrast, if the one-particle Green's function does not exhibit a quasiparticle pole but a power-law relaxation for asymptotically long times, the coherent quasiparticle tunneling can be blocked as a result of the orthogonality catastrophe (5). The observation of a rapidly growing  $c$ -axis resistivity with decreasing temperature in these materials (6) is also consistent with the confinement idea. Note that the observed Fermi surface in photoemission experiments does not establish the Fermi liquid behavior of the normal state; as a counter example, it is only necessary to recall the well-established Luttinger liquid behavior of one-dimensional interacting Fermi systems (7). Thus, the Fermi surface defined as the surface of low-energy excitations in  $\mathbf{k}$ -space that encloses a volume appropriate to the density of electrons can exist in a non-Fermi liquid; in this case, the singularity in the derivative of the electronic occupation number at the Fermi surface will be a power-law instead of a  $\delta$  function.

S. Chakravarty and A. Sudbø, Department of Physics, University of California—Los Angeles, Los Angeles, CA 90024.

P. W. Anderson and S. Strong, Department of Physics, Princeton University, Princeton, NJ 08544.

To treat the superconducting state, we note that the quasiparticle peak, a  $\delta$  function broadened by the thermal as well as the experimental resolution factors, is recovered in this state (8). In contrast, in our picture, the observed normal-state spectral function reflects only a similarly broadened power-law singularity. However, the  $c$ -axis infrared conductivity continues to be small in spite of the development of  $c$ -axis superconductivity (9). Therefore, the quasiparticles are still not mobile in the  $c$  direction, but only in the  $ab$  plane. Thus, we ignore coherent single particle tunneling in the  $c$  direction and consider coherent Josephson pair tunneling which does not suffer the orthogonality catastrophe. We therefore approximate the motion in the  $ab$  plane by the dispersion relation,  $\varepsilon(\mathbf{k}) = -2t[\cos(k_x a) + \cos(k_y a)] + 4t' \cos(k_x a) \cos(k_y a)$ , where  $t = 0.25$  eV and  $t'/t = 0.45$  (10). We have used the electron picture rather than the hole picture.

The gap equation can be derived by considering two close CuO layers described by the BCS (Bardeen-Cooper-Schrieffer) reduced Hamiltonian and coupled by the momentum conserving Josephson pair tunneling term,  $H_J$ , which we write as

$$H_J = - \sum_{\mathbf{k}} T_J(\mathbf{k}) (c_{\mathbf{k}\uparrow}^{(1)\dagger} c_{-\mathbf{k}\downarrow}^{(1)\dagger} c_{-\mathbf{k}\downarrow}^{(2)} c_{\mathbf{k}\uparrow}^{(2)} + \text{h.c.}) \quad (1)$$

where  $c_{\mathbf{k}\uparrow}^{(i)\dagger}$  is the electron creation operator, pertaining to the layer ( $i$ ), of wave vector  $\mathbf{k}$  and spin  $\uparrow$  and h.c. is the Hermitian conjugate. This description is applicable to two-layer compounds, such as YBCO, two-layer Bi2212, or Tl2212; the extension to other types of layered materials is straightforward.

The effective Hamiltonian  $H_J$  is to be understood in the context of renormalization group theory. At high energies, of the order of the bandwidth, the microscopic Hamiltonian should be well described by the band theory that couples the layers by a single particle matrix element,  $t_{\perp}(\mathbf{k})$ , and clearly conserves the wave vector  $\mathbf{k}$ . As the degrees of freedom are integrated out starting at the band edge, the term  $H_J$  is generated. One also generates, in addition, a particle-hole pair hopping term that would be important if we were to describe the magnetic ordering in these systems. Thus, the symmetry of the coefficient in Eq. 1,  $T_J(\mathbf{k})$ , is dictated by the symmetry of  $t_{\perp}(\mathbf{k})$  calculated from band theory. For simplicity, we choose  $T_J(\mathbf{k}) = t_{\perp}(\mathbf{k})^2/t$ . We believe that this is approximately correct in magnitude as well and is certainly what one gets from a second-order perturbative renormalization group analysis. This is also supported by the fact that  $H_J$  reproduces the Josephson energy in conventional superconductors. To see this, it is necessary to

evaluate it only in first-order perturbation theory, for simplicity at  $T = 0$ . The result differs from the conventional answer by a numerical factor close to unity. We do not, however, attempt to continue this perturbative renormalization group analysis all the way to the Fermi energy because the perturbative analysis must eventually break down. Instead, we consider the effective Hamiltonian,  $H_J$ , generated from a partial integration of the degrees of freedom at the starting point of our mean-field theory. Finally, we note that as long as the Coulomb interaction is well-screened, the vertex corrections to  $H_J$  are unimportant. All other effects involving Coulomb interactions are included in the Coulomb pseudopotential parameter,  $\mu^*$ , as in BCS theory.

From the BCS mean-field theory the gap in the quasiparticle spectrum is derived to be

$$\Delta(\mathbf{k}) = T_J(\mathbf{k}) b_{\mathbf{k}} - \sum_{\mathbf{k}'} U_{\mathbf{k},\mathbf{k}'} b_{\mathbf{k}'} \quad (2)$$

where  $b_{\mathbf{k}}^* = \langle c_{\mathbf{k}\uparrow}^{\dagger} c_{-\mathbf{k}\downarrow}^{\dagger} \rangle$ . We have considered the solution  $b_{\mathbf{k}}^{(1)} = b_{\mathbf{k}}^{(2)} \equiv b_{\mathbf{k}}$ . The attractive kernel  $U_{\mathbf{k},\mathbf{k}'}$  is assumed to be due to electron-phonon interaction but could be due to other mechanisms. The sum over  $\mathbf{k}'$  is cut off at an energy  $\omega_D$  from the Fermi energy, where  $\omega_D$  is of the order of the Debye energy. It is crucial, however, that the first term on the right-hand side of Eq. 2 is local in  $\mathbf{k}$ . In fact, the striking properties of this gap equation would not follow if this term were smoothed out in the momentum space over a range comparable to the second term. As stated above, the locality follows from the conservation of the parallel momentum. The role of disorder and inelastic scattering clearly deserves further study, but we believe that  $\mathbf{k}$  is a good quantum number, at least close to  $T_c$ .

The self-consistent equation for  $b_{\mathbf{k}}$  is

$$b_{\mathbf{k}} = - \frac{\chi(\mathbf{k})}{1 - T_J(\mathbf{k})\chi(\mathbf{k})} \sum_{\mathbf{k}'} U_{\mathbf{k},\mathbf{k}'} b_{\mathbf{k}'} \quad (3)$$

where  $b_{\mathbf{k}} = \Delta(\mathbf{k})\chi(\mathbf{k})$ , and the pair susceptibility,  $\chi(\mathbf{k})$ , is  $(1/2E_{\mathbf{k}}) \tanh(E_{\mathbf{k}}/2T)$ . The quasiparticle spectrum is given by  $E_{\mathbf{k}} = \sqrt{\Delta(\mathbf{k})^2 + \varepsilon(\mathbf{k})^2}$ , where, from now on,  $\varepsilon(\mathbf{k})$  will be measured from the chemical potential  $\varepsilon_F$ .

Consider first a  $T_J(\mathbf{k}) = T_J$ , independent of  $\mathbf{k}$  (1). With the simplification that  $U_{\mathbf{k},\mathbf{k}'} = -V$ , ( $|\varepsilon(\mathbf{k})|, |\varepsilon(\mathbf{k}')| < \omega_D$ ), we see that as  $\lambda = N_n(0)V \rightarrow 0$  [ $N_n(0)$  is the normal state density of states at the Fermi energy],  $T_c - T_J/4 \approx (\lambda/1 - \lambda)(T_J/4)$ . The transition temperature  $T_c$  tends to  $T_J/4$  even when  $\lambda \rightarrow 0$ . Moreover, the phonon enhancement is linearly proportional to  $\lambda$ , in contrast to  $T_c \approx \omega_D e^{-1/\lambda}$  in the weak coupling BCS theory. Of course, in the same limit, we expect strong fluctuation

effects in  $\mathbf{k}$ -space, which will act to reduce the mean field transition temperature. These  $\mathbf{k}$ -space fluctuations are easily seen in the pseudospin formalism (12). However, when  $T_J$  is small, we recover the BCS result. As in BCS, the repulsive screened Coulomb interaction modifies this simple result. The expression for the Coulomb pseudopotential,  $\mu^*$  is different, however, and is  $\mu^* \approx \mu[1 + \mu \ln|\varepsilon_F/(\omega_D - T_J/2)|]^{-1}$ , where  $\mu$  is the Coulomb matrix element times the density of states.

Consider the anisotropic equation. The principal symmetry of  $t_{\perp}(\mathbf{k})$  is evident from the electronic structure calculations. The two-dimensional bands of the two layers touch along the line joining  $\Gamma M$ . The point M corresponds to  $(\pi/a, \pi/a)$ . The largest splitting of the hybridized bands of the two layers is seen to be at the point X, which is  $(\pi/a, 0)$ . For clarity, we have chosen the special point notation for a two-dimensional square lattice, instead of the face-centered tetragonal notation. (Small orthorhombic distortions in these materials are unimportant for our discussion.) Thus, if we choose

$$t_{\perp}(\mathbf{k}) = \frac{t_{\perp}}{4} [\cos(k_x a) - \cos(k_y a)]^2 \quad (4)$$

we can reproduce the qualitative features of the Fermi surface quite well; the magnitude  $t_{\perp}$  is in the range 0.1 to 0.15 eV (11) which is also consistent with the magnetic neutron scattering experiments (13). This leads to  $T_J(\mathbf{k}) = (T_J/16)[\cos(k_x a) - \cos(k_y a)]^4$ , where  $T_J = t_{\perp}^2/t$ . Note that the choice  $|\cos(k_x a) - \cos(k_y a)|$  will not agree with the calculated band structure, nor would the choice  $|\cos(k_x a) - \cos(k_y a)|$ , which would produce unwanted cusps in the spectrum. We have also verified the correctness of our choice from a tight-binding calculation.

Solving Eq. 3 at  $T = 0$  gives

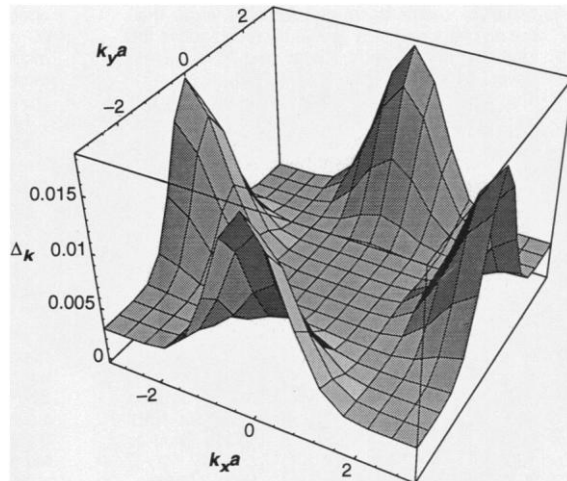
$$\Delta(\mathbf{k}) \left[ 1 - \frac{T_J(\mathbf{k})}{2\sqrt{\varepsilon(\mathbf{k})^2 + \Delta(\mathbf{k})^2}} \right] = \Delta_0 \theta(\omega_D - |\varepsilon(\mathbf{k})|) \quad (5)$$

where  $\Delta_0 = V \sum_{\mathbf{k}'} \Delta(\mathbf{k}') \chi(\mathbf{k}') \theta[\omega_D - |\varepsilon(\mathbf{k}')|]$  must be calculated self-consistently from the full solution  $\Delta(\mathbf{k})$ . To gain some insight, consider the solution on the Fermi surface

$$\Delta(\mathbf{k}_F) = \frac{T_J(\mathbf{k}_F)}{2} + \Delta_0 \quad (6)$$

We see several important features: (i) the gap is highly anisotropic, but has the full symmetry of the crystal. Note that  $\Delta_0$  is not a BCS gap; it contains the enhancing effect of  $T_J(\mathbf{k})$ . (ii) The anisotropy is quadratic in  $t_{\perp}$ , and therefore the gap rapidly acquires pure  $s$ -wave character as  $t_{\perp}$  decreases. (iii) Here, unlike  $d$ -wave, the gap never changes sign. (iv) At the Fermi surface points  $\pm \mathbf{k}_{xF}$

**Fig. 1.** Anisotropic gap  $\Delta(\mathbf{k})$  in electron volts as a function of  $k_x a$  and  $k_y a$  at  $T = 0$ , with  $\lambda = 0.31$  ( $\Delta_0 = 0.003$  eV),  $T_J = 0.03$  eV =  $10\Delta_0$ , and  $\varepsilon_F = -4t' = -0.45$  eV, corresponding to an electron Fermi surface closed around  $\Gamma$ . For clarity of visualization we have omitted the factor  $\theta[\omega_D - |\varepsilon(\mathbf{k})|]$ , which multiplies the gap.



$= \pm k_{yF}$ ,  $T_J(\mathbf{k}_F) = 0$ , and the gap attains its smallest value  $\Delta_0$ . (v) For a Fermi surface closed around the point  $\Gamma$  ( $\varepsilon_F \leq -4t'$ ), the maxima of the gap are in the directions (1,0) and (0,1). The maximum value of the gap is obtained when the Fermi surface includes the points  $(\pi/a, 0)$ ,  $(0, \pi/a)$  and is  $T_J/2 + \Delta_0$ . For larger electron fillings, when the Fermi surface is not closed around the point  $\Gamma$  and does not include the maxima in  $T_J(\mathbf{k})$ , a more complicated structure develops, with the maxima in off-symmetry directions.

We now focus on an electron Fermi surface closed around the  $\Gamma$  point which corresponds to recent experiments on Bi2212 (2). Along the directions (0, 1) or (1, 0), the gap on the Fermi surface is given by

$$\Delta(\mathbf{k}_F) = \Delta_0 + \frac{T_J}{32} \left( 1 - \frac{2t + \varepsilon_F}{4t' - 2t} \right)^4 \quad (7)$$

Thus, it is not difficult to obtain anisotropies similar to those seen in experiments.

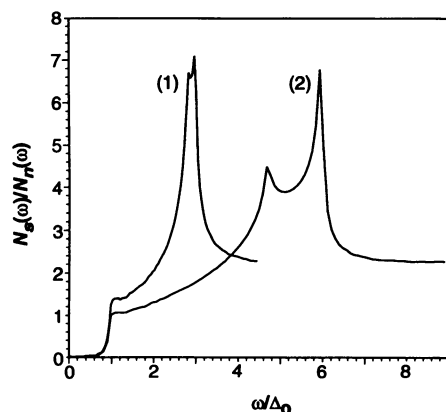


**Fig. 2.** Density of states  $N_s(\omega)/N_n(\omega)$  at  $T = 0$  for  $\varepsilon_F = -4t' = -0.45$  eV, for two sets of parameters: (1)  $T_J = 0.012$  eV,  $\lambda = 0.29$  ( $\Delta_0 = 0.003$  eV); (2)  $T_J = 0.03$  eV,  $\lambda = 0.25$  ( $\Delta_0 = 0.003$  eV). The numerical evaluation of the density of states was carried out by replacing the  $\delta$  function by a Lorentzian of width  $10^{-4}$  eV.

Clearly, the gap anisotropy on the Fermi surface is sensitively dependent on doping. From numerical solutions we have explored the structure of the gap for a range of parameters; a typical example is shown in Fig. 1. Because it is not possible to detect the sign of the gap in angle-resolved photoemission spectroscopy, it is necessary to explore the structure of the gap in more detail and precision, if it is to be distinguished from a  $d$ -wave gap.

We next turn to a brief discussion of the superconducting density of states,  $N_s(\omega) = \frac{1}{2} \sum_{\mathbf{k}} \delta(\omega - E_{\mathbf{k}})$ , obtained from the quasiparticle spectrum  $E_{\mathbf{k}}$  at  $T = 0$ . We have calculated  $N_s(\omega)$  for a variety of parameters; an example is shown in Fig. 2. The low-energy features are as follows. At the lower gap edge,  $\Delta_0$ ,  $N_s(\omega)$  has a step discontinuity if  $T_J \neq 0$ , which can be proven analytically. There are also logarithmic singularities (proven analytically) at higher energies (see Fig. 2) similar to the logarithmic singularities in the  $d$ -wave den-

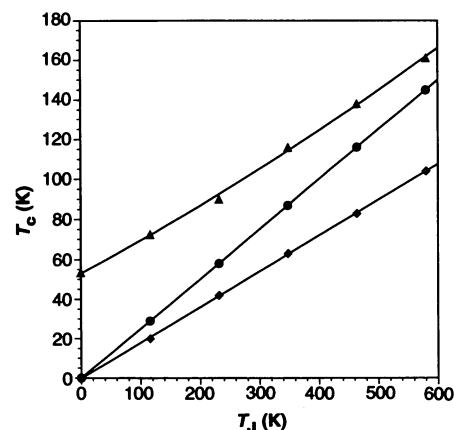


**Fig. 3.** Critical temperature  $T_c$  as a function of  $T_J$ ;  $\omega_D = 0.02$  eV: ( $\Delta$ )  $\varepsilon_F = -4t' = -0.45$  eV,  $N_n = 2.5$ /eV-spin,  $\lambda = 0.625$ ; ( $\circ$ )  $\varepsilon_F = -4t' = -0.45$  eV,  $N_n = 2.5$ /eV-spin,  $\lambda = 0.0625$ ; ( $\diamond$ )  $\varepsilon_F = -2.67t' = -0.3$  eV,  $N_n = 0.8$ /eV-spin,  $\lambda = 0.2$ .

sity of states. Clearly, these integrable singularities smoothed further by the observed inelasticity (14) cannot give rise to the Hebel-Slichter peak in the nuclear magnetic relaxation rates. The absence of the Hebel-Slichter peak is an important distinguishing feature of the high-temperature superconductors.

The critical temperature  $T_c$  can be determined from Eq. 3. Note that one can obtain a lower bound on  $T_c$  by neglecting the phonon enhancement term in the gap equation. We find  $T_c \geq [T_J(\mathbf{k})/4]_{\max}$ . When the Fermi surface is closed around  $\Gamma$  (that is,  $\varepsilon_F \leq -4t'$ ), this leads to

$$T_c = \frac{T_J}{64} \left( 1 - \frac{2t + \varepsilon_F}{4t' - 2t} \right)^4 \quad (8)$$

However, when the Fermi surface is open around  $\Gamma$  (that is,  $\varepsilon_F \geq -4t'$ ), we find

$$T_c = \frac{T_J}{64} \left( 1 + \frac{2t - \varepsilon_F}{4t' + 2t} \right)^4 \quad (9)$$

Remarkably, the lower bound,  $T_c = T_J/4$ , when  $\varepsilon_F = -4t'$ , is identical to the isotropic estimate when  $T_J \gg V$ . The numerical evaluation of  $T_c$  is shown in Fig. 3 for typical sets of parameters.

It is clear from above that  $T_c$  is highest (not only the lower bound) when  $\varepsilon_F = -4t'$  but falls away from this doping. A high value of  $T_c$  is obtained when the maxima of  $T_J(\mathbf{k})$  are included within the shell  $2\omega_D$  of the Fermi surface, and has nothing to do with the existence of van Hove singularities in the density of states. Note that the lower bound does not even involve the density of states at the Fermi surface. For lower  $T_c$  materials,  $T_J$  plays a less important role and  $T_c$  begins to be increasingly controlled by the phonon coupling, thereby reaching the standard BCS value. Therefore, for materials with highest  $T_c$ 's,  $T_J$  dominates and the isotope effect is expected to be small. Conversely, materials with low  $T_c$ 's should exhibit a normal isotope effect. This is in agreement with our earlier isotropic estimate which showed that when  $T_J$  dominated, even the phonon contribution, linearly proportional to  $\lambda$ , is independent of isotopic substitution. On the other hand, when  $T_J$  was small, we had the BCS result corresponding to normal isotope effect. It is now evident that the dispersion of  $t_{\perp}(\mathbf{k})$  is essential in producing this crossover in the isotope effect.

From the gap equation, it is possible to prove that as long as  $\Delta_0 \neq 0$ , all the Fourier modes of  $\Delta(\mathbf{k})$  vanish at the same temperature  $T_c$ . It is also important to note that a value of  $T_J \approx 400$  K used to obtain a  $T_c$  of the order of 100 K is an underestimate from what we know about  $t_{\perp}$ ;  $T_J$  could be as large as 1000 K. Of course, fluctuation effects, not included in our mean field theory, will reduce  $T_c$ .

In the present report we have tried to be as quantitative as possible for two-layer materials. The pairing mechanism within a given layer was assumed to be BCS-type electron-phonon interaction because we believe this to be the most realistic possibility. In previous work (1, 15) we gave a simple formula for  $T_j$  which can be used to generalize to other materials with variable layer numbers (including single-layer compounds for which  $T_j$  characterizes the coupling between the CuO layers in adjacent unit cells), and have shown that it yields a good heuristic fit to  $T_c$  versus number of layers for Bi and Tl one-, two-, and three-layer materials as well as a prediction for  $\infty$ -layer materials. This leads to a near zero  $T_c$  for Bi one-layer materials, but to a  $T_c \sim 60$  to 70 K for Tl one-layer materials [ $T_j$  is considerably larger in this case (16)]. The fit to the recently discovered Hg-based materials (17) is also satisfactory. A prediction, based on the present ideas, is that  $\text{La}_{2-x}\text{Sr}_x\text{CuO}_4$  as well as  $\text{Nd}_{2-x}\text{Ce}_x\text{CuO}_4$  should exhibit roughly isotropic gaps because  $t_{\perp}(\mathbf{k})$  is not very anisotropic within tight-binding approximation.

## REFERENCES AND NOTES

1. P. W. Anderson, in *Superconductivity, Proceedings of the ICTP Spring College in 1992*, P. Butcher and Y. Lu, Eds. (World Scientific, Singapore, in press).
2. Z.-X. Shen *et al.*, *Phys. Rev. Lett.* **70**, 1553 (1993).
3. V. J. Emery, *Ann. Phys. N.Y.* **28**, 1 (1964).
4. P. W. Anderson, *Science* **256**, 1526 (1992); C. M. Varma *et al.*, *Phys. Rev. Lett.* **63**, 1996 (1989); *ibid.* **64**, 497 (1990), erratum.
5. G. D. Mahan, *Many Particle Physics* (Plenum, New York, 1990). For a recent discussion of the orthogonality catastrophe, see P. W. Anderson (*Math. Rev.*, in press) and references therein. If we adiabatically decouple the motion of an electron perpendicular to the layers, for each  $\mathbf{k}$ , one can construct a two-state system coupled to the bath of in-plane excitations. In a non-Fermi liquid any attempt to tunnel between the layers will significantly disturb all the electrons in the system. Thus, the tunneling matrix element will be multiplied by a overlap matrix element involving  $N(N \rightarrow \infty)$  electrons, which can vanish depending on the spectral density of the bath of excitations; see S. Chakravarty, *Phys. Rev. Lett.* **49**, 681 (1982), and A. J. Leggett *et al.*, *Rev. Mod. Phys.* **59**, 1 (1987). Here, this would happen if the spectral function corresponding to the one-particle Green's function satisfies the homogeneity relation  $A(\Lambda\omega, \Lambda k) = \Lambda^{\alpha-1} A(\omega, k)$  and the exponent  $\alpha \geq 1$ . There are, however, logarithmic corrections as  $\alpha \rightarrow 1$ . The value  $\alpha = 1$  will lead to a precise linear  $T$  dependence of the in-plane resistivity in these materials. We emphasize that the physical effect will not be very different even if  $\alpha < 1$  provided that  $T$  is larger than the crossover temperature  $t_{\perp}(t_{\perp}/W)^{\alpha/(1-\alpha)}$ , where  $W$  is of the order of the bandwidth. For another derivation, see P. W. Anderson, in preparation.
6. See, for example, B. Batlogg in *High Temperature Superconductivity*, K. S. Bedell *et al.*, Eds. (Addison-Wesley, Redding, MA, 1990). The observation, in some samples, of a  $c$ -axis resistivity which follows a linear (or more complex) temperature dependence does not imply coherent tunneling of quasiparticles between the planes. This behavior can arise if the hopping rate between the layers, renormalized by the coupling to the intralayer excitations, is smaller than the temperature; a crucial point is that the magnitude of the  $c$ -axis resistivity seems to be considerably larger than the  $ab$  plane resistivity, generally much above the Mott limit at  $T_c$ ; see N. Kumar and A. M. Jayanavar, *Phys. Rev. B* **45**, 5001 (1992).
7. That  $\mathbf{k}_F$  remains unshifted in the Luttinger model was first pointed out by D. C. Mattis and E. H. Lieb, *J. Math. Phys.* **6**, 304 (1965). This follows from a counting argument because there are no level crossings. Such a counting argument is independent of the dimensionality of the electron gas.
8. C. G. Olson *et al.*, *Science* **245**, 731 (1989); D. S. Dessau *et al.*, *Phys. Rev. Lett.* **66**, 2160 (1991).
9. K. Tamasaku, Y. Nakamura, S. Uchida, *Phys. Rev. Lett.* **69**, 1455 (1992).
10. See, for example, J. Yu and A. J. Freeman, *J. Phys. Chem. Solids* **52**, 1351 (1991).
11. See, for example, S. Massida, J. Yu, A. J. Freeman, *Physica C* **152**, 251 (1988); M. S. Hybertsen and L. F. Mattheiss, *Phys. Rev. Lett.* **60**, 1661 (1988); H. Krakauer and W. E. Pickett, *ibid.*, p. 1665.
12. P. W. Anderson, *Phys. Rev.* **112**, 1900 (1958).
13. J. Tranquada *et al.*, *Phys. Rev. B* **40**, 4503 (1989); J. Tranquada *et al.*, *ibid.* **46**, 5561 (1992). Note that for  $O_{6g}$ , the optic mode in the spin wave spectrum due to bilayers was not observed up to 60 meV. For  $O_{6g}$ , some indication of the optic mode has been observed for energies greater than 40 meV.
14. D. A. Bonn *et al.*, *Phys. Rev. Lett.* **68**, 2390 (1991).
15. J. M. Wheatley, T. C. Hsu, P. W. Anderson, *Phys. Rev. B* **37**, 5897 (1988).
16. We argue this on the basis of the band structure calculations of D. J. Singh and W. E. Pickett [*Physica C* **203**, 193 (1992)] and D. R. Hamann and L. F. Mattheiss [*Phys. Rev. B* **38**, 5138 (1988)].
17. A. Schilling *et al.*, *Nature* **363**, 56 (1993); S. N. Putilin *et al.*, *ibid.* **362**, 226 (1993).
18. We thank E. Abrahams, W. E. Pickett, and Z.-X. Shen for useful discussions. This work was supported in part by the National Science Foundation, DMR-9104873 (P.W.A. and S.S.), DMR-9220416 (S.C.), and in part by the Office of Naval Research, ONR-92J1101 (S.C. and A.S.). S.C. also thanks the John Simon Guggenheim Memorial Foundation for support through a fellowship and S.S. the AT&T Bell Laboratories for a Ph.D. scholarship.

2 April 1993; accepted 28 May 1993

## How Fish Power Swimming

Lawrence C. Rome,\* Douglas Swank, David Corda

It is thought that fish generate the power needed for steady swimming with their anterior musculature, whereas the posterior musculature only transmits forces to the tail and does negative work. Isolated red muscle bundles driven through the length changes and stimulation pattern that muscles normally undergo during steady swimming showed the opposite pattern. Most of the power for swimming came from muscle in the posterior region of the fish, and relatively little came from the anterior musculature. In addition, the contractile properties of the muscle along the length of the fish are significantly adapted to enhance power generation.

To maintain a constant velocity through a viscous medium, a body must generate mechanical power. In fish, the mechanical power is generated by muscle. It is thought that during typical swimming (caudal fin propulsion), most of the power is exerted on the water by the tail (1). Therefore, the power must either be generated by the musculature adjacent to the tail or be somehow transmitted to the tail. A combination of kinematics, electromyography, and mathematical modeling led to the current theory that there is a systematic shift in muscle function along the length of the fish. Specifically, the anterior musculature generates most of the power (by shortening contractions, which produce positive work), and the posterior musculature only transmits force to the tail [by lengthening

contractions, in which the muscle develops tension but is lengthened rather than shortened; this greatly stiffens the muscle (2) but produces negative work (3)]. Thus, by analogy (4), the anterior muscle is the "motor," the tail is the "propeller," and the lengthening posterior muscle is the "drive shaft." Although this hypothesis is widely accepted, it has never been rigorously tested.

We therefore measured the power that was generated by muscle at various places along the length of the fish. Power generated by muscle is the product of tailbeat frequency and the work per tailbeat (that is,  $Fd\ell$ , where  $F$  is force and  $\ell$  is length, integrated over the tailbeat cycle). Thus, in theory, one need only measure the instantaneous force production and length change of the muscle during the tailbeat cycle to determine power production at a particular position on the fish. Although muscle length changes can be measured during swimming, it is not experimentally possible to measure force production directly (fish musculature precludes the use of an in vivo force transducer). However, because the force produced by muscle is a function of

L. C. Rome and D. Corda, Department of Biology, University of Pennsylvania, Philadelphia, PA 19104, Coastal Research Center, Woods Hole Oceanographic Institution, and Marine Biological Laboratories, Woods Hole, MA 02543.  
D. Swank, Department of Physiology, University of Pennsylvania, Philadelphia, PA 19104.

\*To whom correspondence should be addressed.